Citation: Cell Death and Disease (2011) 2, e191; doi:10.1038/cddis.2011.73

www.nature.com/cddis

The organotelluride catalyst LAB027 prevents colon cancer growth in the mice

R Coriat[1,3], W Marut[1,3], M Leconte[1], LB Ba[2], A Vienne[1], C Chéreau[1], J Alexandre[1], B Weill[1], M Doering[2], C Jacob[2], C Nicco[1,3] and F Batteux*[,1,3]

Organotellurides are newly described redox-catalyst molecules with original pro-oxidative properties. We have investigated the *in vitro* and *in vivo* antitumoral effects of the organotelluride catalyst LAB027 in a mouse model of colon cancer and determined its profile of toxicity *in vivo*. LAB027 induced an overproduction of H_2O_2 by both human HT29 and murine CT26 colon cancer cell lines *in vitro*. This oxidative stress was associated with a decrease in proliferation and survival rates of the two cell lines. LAB027 triggered a caspase-independent, ROS-mediated cell death by necrosis associated with mitochondrial damages and autophagy. LAB027 also synergized with the cytotoxic drug oxaliplatin to augment its cytostatic and cytotoxic effects on colon cancer cell lines but not on normal fibroblasts. The opposite effects of LAB027 on tumor and on non-transformed cells were linked to differences in the modulation of reduced glutathione metabolism between the two types of cells. In mice grafted with CT26 tumor cells, LAB027 alone decreased tumor growth compared with untreated mice, and synergized with oxaliplatin to further decrease tumor development compared with mice treated with oxaliplatin alone. LAB027 an organotelluride catalyst compound synergized with oxaliplatin to prevent both *in vitro* and *in vivo* colon cancer cell proliferation while decreasing the *in vivo* toxicity of oxaliplatin. No *in vivo* adverse effect of LAB027 was observed in this model.

Cell Death and Disease (2011) **2,** e191; doi:10.1038/cddis.2011.73; published online 11 August 2011
Subject Category: Cancer

All living organisms need to maintain a healthy intracellular redox balance in order to survive and to proliferate.[1] Reactive oxygen species (ROS) are natural by-products of aerobic metabolism whose production correlates with normal cell proliferation through the activation of growth-related signaling pathways.[2] Exposure to low levels of ROS can stimulate the growth of many types of mammalian cells, whereas scavengers of ROS suppress normal cell proliferation in human and rodent fibroblasts.[3,4] Furthermore, growth factors trigger the production of hydrogen peroxide (H_2O_2) that leads to mitogen-activated protein kinase activation and DNA synthesis, a phenomenon inhibited by antioxidant molecules.[5,6] Several observations suggest that ROS also participate in carcinogenesis. First, ROS production is increased in cancer cells, and an oxidative stress can induce DNA damages that lead to genomic instability and possibly stimulate cancer progression.[7] Second, elevated ROS levels are responsible for the activation of transcription factors, such as NF-κB and AP-1 during tumor progression.[8] Several studies have shown that different types of cancer cells such as colon, liver, lung, kidney, prostate and skin cancer cells[9–11] display a high proliferation rate associated with an increased endogenous production of ROS and a downregulation of their antioxidant enzymatic systems.

On the other hand, ROS can also induce the apoptosis/necrosis of cancer cells. Indeed, most anticancer drugs kill their target cells, at least in part, through the generation of high amounts of intracellular ROS that stimulate pro-apoptotic signal molecules.[12,13] Several anticancer agents, such as 5-fluorouracil,[14] platinum,[9,12] arsenic trioxide,[15] paclitaxel,[16] and anthracyclines[17] increase the intra-cellular levels of ROS. Tumor cells generate higher levels of ROS compared with normal cells and are therefore more sensitive to the additional oxidative stress caused by anticancer agents.[9,12,18]

Cells also contain a variety of free radical scavenging systems that protect them from the effects of drugs that generate ROS. Catalase and glutathione peroxidase are enzymes that detoxify H_2O_2. High levels of reduced glutathione, the cofactor of glutathione peroxidase, have been associated with the multidrug resistance phenotype in tumor cells.[19] Therefore, compounds that target such protective mechanisms could enhance the activity of anticancer agents and reverse the multidrug resistance phenotype. For example, buthionine sulfoximine (BSO), a glutathione synthesis inhibitor, can increase the cytotoxicity of melphalan by preventing glutathione peroxidase activity.[20] Conversely, *N*-acetylcysteine protects normal cells from the cytotoxic effects of anticancer drugs by preventing the elevation of

[1]Université Paris Descartes, Faculté de Médecine, Hôpital Cochin, Assistance Publique-Hôpitaux de Paris (AP-HP), Laboratoire d'immunologie, EA 1833, Paris, France and [2]Division of Bioorganic Chemistry, School of Pharmacy, Saarland University, PO Box 151150, D-66123, Saarbruecken, Germany
*Corresponding author: F Batteux, Laboratoire d'Immunologie, UPRES EA 1833, Université Paris Descartes, 24 rue du faubourg St. Jacques, 75679 Paris cedex 14, France. Tel: +33 015 841 2007; Fax: +33 015 841 2008; E-mail: frederic.batteux@cch.aphp.fr
[3]These authors contributed equally to this work.
Keywords: tellurium; colon cancer; mice; reactive oxygen species; oxaliplatin
Abbreviations: DHE, dihydroethidium; H2DCFDA, dichlorodihydrofluorescein diacetate; H_2O_2, hydrogen peroxide; ROS, reactive oxygen species
Received 25.11.10; revised 27.5.11; accepted 14.6.11; Edited by V De Laurenzi

intracellular H_2O_2 through its reductive properties.[9] SOD enzymes can also affect tumor cell proliferation via their effects on peroxide levels. Thus, the overexpression of SOD in human cancer cell lines or the use of nonpeptidyl mimic of SOD increases H_2O_2 production and reduces tumor growth.[9,16,21,22]

Killing cancer cells through the oxidative stress may require compounds that generate ROS and, more appropriately, catalysts that convert the intracellular ROS into a cocktail of cytotoxic chemical species that selectively kills cancer cells.[18,23] Compounds that contain quinones and tellurium are cytotoxic at low concentrations.[24] The LAB027 compound that associates a quinone core along with two tellurium atoms can thus be considered as the prototype of pro-oxidative tellurium compounds. However, LAB027 as well as the other multifunctional redox catalysts synthesized so far have always been tested alone and *in vitro*.

Colon cancer cells are highly sensitive to the oxidative stress[18] and are currently treated by 5FU, oxaliplatin and irinotecan, that generate an intracellular stress in cancer cells. The capacity of organotelluride catalysts to generate an intracellular oxidative burst alone and in combination with a pro-oxidative cytotoxic drug, prompted us to test these molecules against colon cancer *in vitro* and *in vivo*. Therefore, we investigated the antitumoral activity of the organotelluride catalyst LAB027 alone and in combination with oxaliplatin *in vitro* and *in vivo* in an animal model of colon cancer. Because of the therapeutic potential of this compound, an evaluation of its profile of toxicity profile has also been performed.

Results

LAB027 exerts pro-oxidative effects *in vitro*. Incubation of mouse CT26 and human HT29 colon cancer cell lines with increasing amounts of LAB027, dose-dependently increased the production of $O_2^{\bullet -}$ (CT26: $P<0.05$ with 2 μM LAB027; HT29: $P<0.05$ with 1 μM LAB027) (Figure 1). A dose-dependent increase in the production of H_2O_2 was also observed (CT26: $P<0.05$ with 2 μM LAB027; HT29: $P<0.05$ with 2 μM LAB027) (Figure 1). Incubation of NIH3T3 fibroblasts with increasing amounts of LAB027 had no effects on the production of $O_2^{\bullet -}$ ($P=$NS), but dose dependently increased the production of H_2O_2 by 500% (NIH3T3: $P<0.05$ with 1 μM LAB027) (Figure 1). Incubation of W138 fibroblasts with increasing amounts of LAB027 had no effects on the production of $O_2^{\bullet -}$ ($P=$NS), but dose-dependently increased the production of H_2O_2 by 260% (W138: $P<0.05$ with 1 μM LAB027) (Figure 1).

LAB027 alters the activities of antioxidant enzymes *in vitro*. Incubation of CT26 and HT29 cells with increasing amounts of LAB027 did not significantly alter SOD, catalase and glutathione reductase activities ($P=$NS compared with untreated cells) (Supplementary Figure 2). By contrast, incubation of NIH3T3 or W138 fibroblasts with increasing amounts of LAB027 dose-dependently increased the production of SOD ($P<0.001$ for NIH3T3 and $P<0.001$ for W138 with 4 μM LAB027) and glutathione reductase activities ($P<0.001$ for NIH3T3 and $P<0.001$ for W138 with 4 μM LAB027) *versus* untreated cells (Supplementary Figure 2) but had no effect on catalase levels.

LAB027 exerts cytostatic and cytotoxic effects *in vitro*. Incubation of CT26 or HT29 cells with increasing amounts of LAB027 dose-dependently decreased their proliferative rates and their viability (Figures 2a and b). At 1 μM, LAB027 decreased CT26 and HT29 proliferation rates by 54% and 57%, respectively ($P<0.001$ for CT26 and $P<0.001$ for HT29), and decreased their viability by 31 and 27%, respectively ($P<0.001$ for CT26 and $P<0.05$ for HT29). Incubation of NIH3T3 or W138 fibroblasts with increasing amounts of LAB027, dose-dependently decreased their proliferation rates and their viability. At

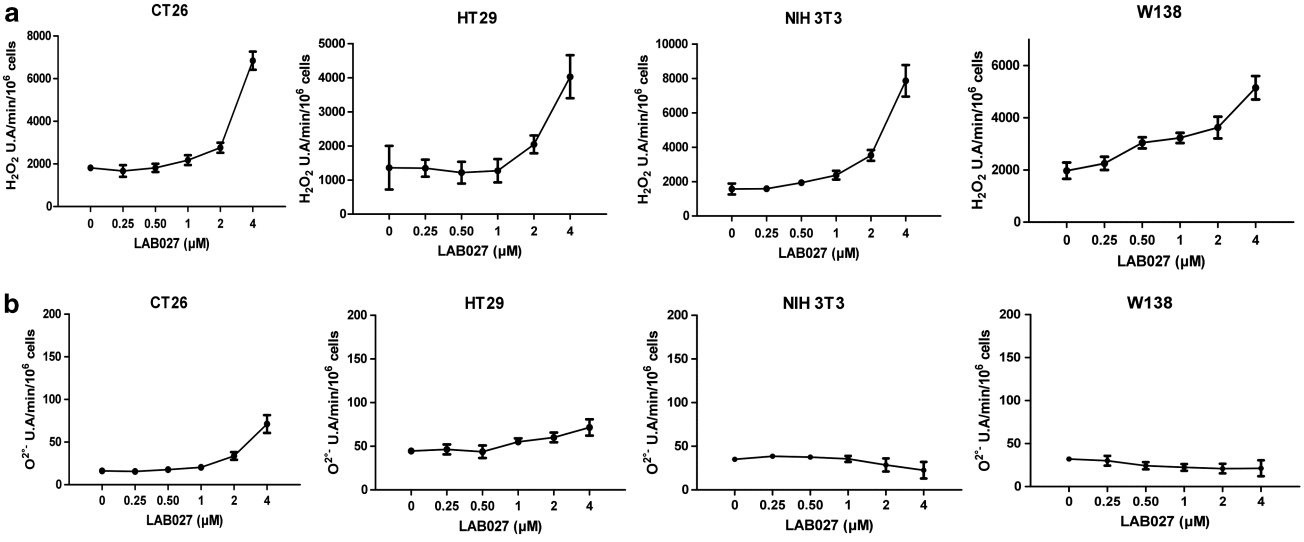

Figure 1 Production of hydrogen peroxide (**a**) and of superoxide anions (**b**) by CT26, HT29, NIH3T3 and W138 cells incubated with increasing concentrations of LAB027. Results are the mean ± S.E.M. of three experiments performed in triplicates

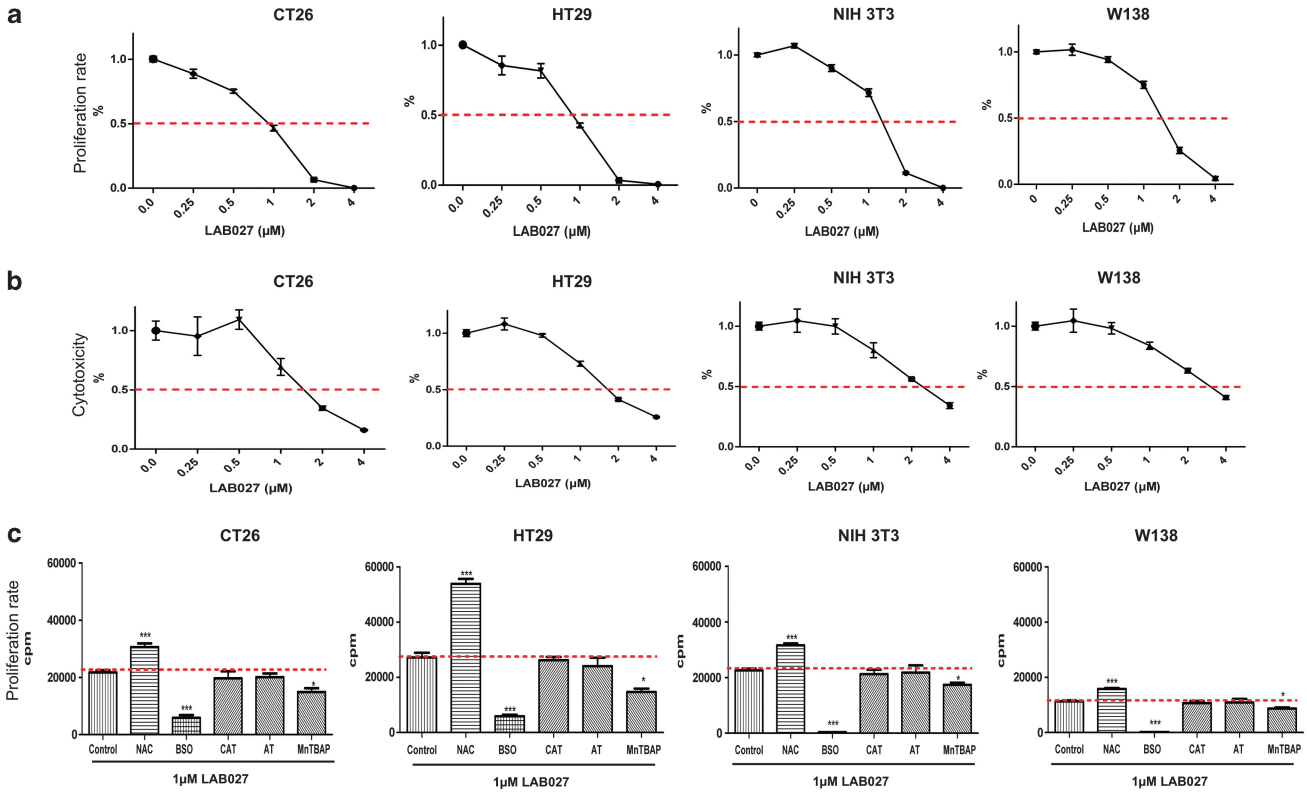

Figure 2 Proliferation rates (**a**) and cytotoxicity (**b**) of CT26, HT29, NIH3T3 and W138 cells incubated with various concentrations of LAB027. Results are the mean ± S.E.M. of three experiments performed in triplicates. Proliferation (**c**) of CT26, HT29, NIH3T3 and W138 cell lines following incubation with 1 μM LAB027 alone, or associated with either 400 μM *N*-acetylcysteine, 400 μM DL-buthionine-(S,R)-sulfoximine (BSO), 200 μM 3-amino-1,2,4-triazole (AT), 50 units/ml catalase PEG (CAT) or with 100 μM MnTBAP. Cellular proliferation was mesured by thymidine incorporation. Error bars represent S.E.M.

1 μM LAB027 decreased NIH3T3 and W138 proliferation rates by 28 and 25%, respectively ($P<0.001$ for NIH3T3 and $P<0.001$ for W138), and decreased their viability by 20 and 17%, respectively ($P<0.05$ for NIH3T3 and $P<0.05$ for W138) (Figures 2a and b). LAB027 was significantly more cytostatic and cytotoxic in CT26 and in HT29 tumor cells lines compared with non-tumoral NIH3T3 and W138 fibroblasts (cytostatic effect of 1 μM LAB027: CT26 *versus* NIH3T3, $P<0.001$; CT26 *versus* W138, $P<0.001$; HT29 *versus* NIH3T3, $P<0.001$; HT29 *versus* W138, $P<0.001$; cytotoxic effect of 2 μM LAB027: CT26 *versus* NIH3T3, $P<0.001$; CT26 *versus* W138, $P<0.001$; HT29 *versus* NIH3T3, $P<0.001$; HT29 *versus* W138, $P<0.001$). The antiproliferative effect of 1 μM LAB027 on CT26, HT29 NIH3T3 and W138 cells was significantly abrogated *in vitro* by 400 μM *N*-acetylcysteine ($P<0.05$; $P<0.02$; $P<0.05$; $P<0.05$, respectively). By contrast, the SOD mimic MnTBAP that produces H_2O_2 through the dismutation of $O_2^{\bullet -}$, significantly increased the antiproliferative activities of 1 μM LAB027 on CT26 ($P<0.05$), on HT29 ($P<0.02$), on NIH3T3 ($P<0.05$) and on W138 ($P<0.05$). Incubation of 1 μM LAB027 with the gamma-glutamylcysteine synthetase inhibitor BSO that depletes intracellular GSH, significantly augmented the cytotoxicity of LAB027 in all cell lines ($P<0.001$). By contrast, blocking catalase by aminotriazol or increasing its intracellular levels by incubation with PEG-catalase had no effects on cell survival or proliferation whatever the cell type considered (Figure 2c).

Cytotoxic pathways engaged by LAB027. To determine the pathway through which LAB027 promotes tumor cell death, we examined by western blot the cleavage of caspase-3 and caspase-8 proteins 24 h after incubation of HT29 tumor cells with increasing amounts of LAB027. Although the expression of cleaved caspase-8 fragments was dose-dependently upregulated in HT29 cells treated with LAB027, no caspase-3 cleavage was observed in LAB027-treated HT29 cells at any concentration tested (Figure 3a). Incubation of HT29, CT26 or NIH 3T3 cells with either caspase-3-specific inhibitor Ac-DEVD-FMK, or with caspase-8 inhibitor Z-IETD-FMK or with the broad-spectrum caspase inhibitor Z-VAD-FMK along with LAB027 did not modify the cytotoxic effects of LAB027 (Figure 3b), whereas the latter two caspases inhibitors effectively inhibited caspase-8 cleavage at the concentration tested (not shown). Early intracellular events that occur during cell death are associated with mitochondrial changes mediated by members of the Bcl-2 family of proteins, including antiapoptotic Bcl-2, Bcl-xL and pro-apoptotic Bax, Bad proteins. In addition, treatment of HT29 cells with LAB027 triggered an autophagic process (Figure 3) as demonstrated by ATG8 induction and cleavage, and by autophagic

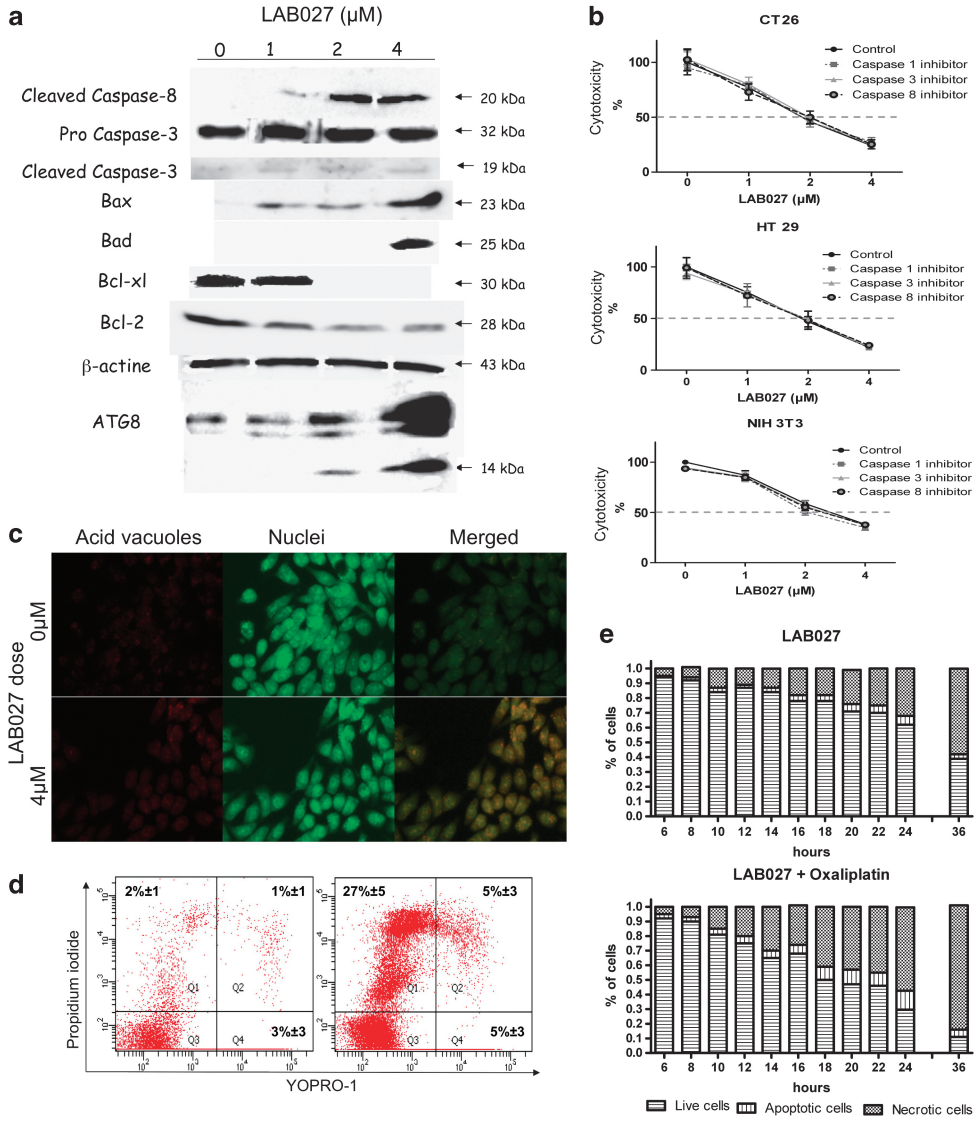

Figure 3 Pro-apoptotic effects of LAB027 (**a**). HT29 cells were treated or not with increasing concentrations of LAB027 for 24 h. Expressions of cleaved caspase-8, pro-caspase-3 and cleaved caspase-3, Bax, Bad, Bcl-xL, Bcl-2 and ATG8 proteins were analyzed by western blot. Proliferation rates (**b**) of CT26, HT29 and NIH3T3 cells incubated with various concentrations of LAB027 alone or associated with either 40 μM DEVD-FMK (caspase-3 inhibitor) or 40 μM IETD-FMK (caspase-8 inhibitor) 40 μM ZVAD-FMK (broad-spectrum caspase inhibitor). Results are means ± S.E.M. of three independent experiments. (**c**) Immunofluorescence microscopy of HT29 cells stained with acridine orange and treated for 24 h or not with 4 μM LAB027. An increased number of cells with stained acidic vesicular organelles (orange fluorescence) in 4 μM LAB027 treated cells was observed. (**d**) Fluorescence-activated cell sorting analysis of cell death. Apoptosis/necrosis was analyzed by flow cytometry using the Membrane Permeability/Dead Cell Apoptosis Kit with YO-PRO-1 and Propidium iodide on HT29 treated (right panel) or not (left panel) with 4 μM LAB027 for 24 h. Necrotic cells are PI positive and YO-PRO-1 positive or negative. Apoptotic cells are PI negative and YO-PRO-1 positive. Viable cells are negative for both dyes. One representative experiment of three is shown. (**e**) Kinetic apoptosis/necrosis evolution in HT29 cells treated with 4 μM LAB027 alone or with oxaliplatin 0.5 μM

vacuolization as demonstrated by acridine orange staining. To clarify the mode of cell death, LAB027-treated HT29 cells were stained with PI and YOPRO-1. After 24-h incubation with 4 μM LAB027, 5% ± 3 HT29 were positive for YOPRO-1 alone and 33% ± 7 HT29 were positive for PI alone or with YOPRO-1 showing a necrotic process (Figure 3d). A kinetic analysis of the mode of cell death between 6 and 24 h indicated that LAB027 induces cell death mainly through a necrotic process (Figure 3e).

LAB027 synergized with oxaliplatin to trigger ROS production and exert cytostatic effects on colon cancer cell lines *in vitro*. Co-incubation of CT26 or HT29 cells with 5 or 0.5 μM oxaliplatin and increasing concentrations of LAB027, augmented the production of H_2O_2 up to 323% (CT26) or 1215% (HT29) at the highest concentration of LAB027 tested. By contrast, co-incubation of mouse NIH3T3 fibroblasts with 5 μM oxaliplatin and LAB027 did not augment the production of H_2O_2 *versus* oxaliplatin alone (Figure 4). Moreover, co-incubation of CT26, HT29 or NIH3T3 cells with oxaliplatin (5 μM with CT26 cells and NIH3T3 cells; 0.5 μM with HT29 cells) with increasing concentrations of LAB027 did not augment the production of $O_2^{\bullet -}$ *versus* oxaliplatin alone (Figure 4).

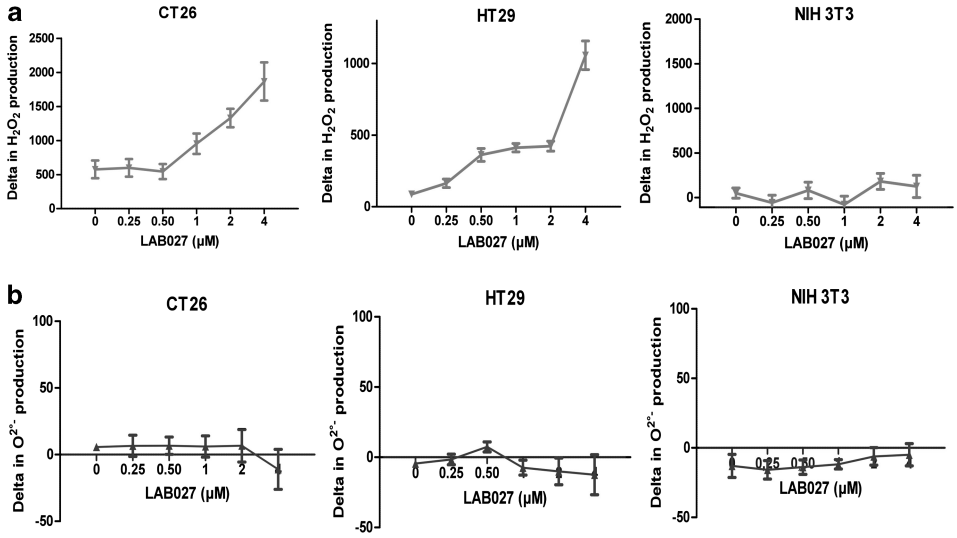

Figure 4 Production of hydrogen peroxide (**a**) and superoxide anions (**b**) by oxaliplatin-treated CT26, HT29 and NIH3T3 cells incubated with increasing concentrations of LAB027. Differences (delta) in H_2O_2 production (**a**) and in $O_2^{\bullet-}$ production (**b**) between oxaliplatin-treated cells and untreated cells are shown. Results are the mean ± S.E.M. of three experiments performed in triplicate

Incubation of HT29 colon cancer cells with 1 μM LAB027 along with 0.5 μM oxaliplatin significantly increased the antiproliferative potential of LAB027 by 31% ($P<0.05$) and the antiproliferative potential of oxaliplatin by 23% ($P<0.05$). By contrast, incubation of mouse NIH3T3 fibroblasts with 1 μM LAB027 along with 5 μM oxaliplatin did not significantly modify the antiproliferative potential of LAB027 ($P=0.68$) or of oxaliplatin ($P=0.85$) administered alone (Figure 5). A kinetic analysis of the mode of cell death induced by co-incubation of LAB027 with oxaliplatin was performed on HT29 cells. The percentages of necrotic cells among apoptotic + necrotic cells were 81%, 84% and 84% after 6, 12 and 24 h incubation, respectively, with LAB027 alone compared with 60, 80 and 83% after 6, 12 and 24 h incubation, respectively, with oxaliplatin + LAB027 (Figure 3e).

Imbalance of GSH metabolism in tumor cells. In normal NIH3T3 cells, increasing the oxidative stress by incubation with 4 μM LAB027 augmented intracellular GSH levels by 311% (Figure 5). Adding 5 μM oxaliplatin to LAB027, further increased GSH synthesis by 80%. Interestingly, incubating CT26 or HT29 colon cancer cells with LAB027 alone or in association with oxaliplatin failed to increase GSH synthesis (Figure 5). In order to determine whether this phenomenon was linked to a differential effect of LAB027 on GSH efflux in normal and tumor cells, we measured the GSH released from CT26, HT29 or NIH3T3 upon incubation with increasing concentrations of LAB027 alone or in association with oxaliplatin. Increasing concentrations of LAB027 significantly induced GSH release, but no difference was observed between normal and tumor cells (Supplementary Figure 3).

Co-incubation of oxaliplatin and LAB027 with the glutathione reductase inhibitor BSO that depletes the cells in reduced glutathione, significantly increased the antiproliferative potential of oxaliplatin + LAB027 in all cell lines ($P<0.001$). In addition, incubation with NAC, a precursor of GSH significantly increased cell proliferation ($P<0.001$ for HT29 and CT26 and $P<0.05$ for 3T3). By contrast, blocking catalase with aminotriazol or increasing its intracellular levels with PEG-catalase had no effect on cell survival and proliferation whatever the cell type considered (Figure 5).

Effect of LAB027 on the growth of CT26 tumor cells implanted in mice treated with oxaliplatin. To determine whether LAB027 could inhibit tumor growth *in vivo*, we treated mice bearing CT26 tumors with either oxaliplatin or LAB027, or with the association of oxaliplatin and LAB027 (Figure 6a). Mice treated with oxaliplatin alone developed significantly smaller tumors than untreated mice (–58%, $P<0.001$ *versus* untreated mice on day 27). LAB027 also inhibited tumor growth when administered alone (−25% on day 27, $P<0.05$ *versus* untreated mice). Mice treated simultaneously with LAB027 and oxaliplatin had significantly smaller tumors than untreated mice on day 27 (−75%, $P<0.001$). Furthermore, the administration of LAB027 amplified the antitumor effect observed with oxaliplatin alone (−41% *versus* oxaliplatin-treated mice, $P<0.05$ on day 27). In order to determine whether the immune system has a role in the antitumoral effects induced by LAB027 alone or in combination with oxaliplatin, we performed the same experiment using immunodeficient SCID mice. In SCID mice implanted with CT26, LAB027 inhibited tumor growth when administered alone (−24% at day 27, $P<0.05$ *versus* untreated mice). SCID mice treated simultaneously with LAB027 and oxaliplatin had significantly smaller tumors than untreated mice at day 27 (−78%, $P<0.001$). The administration of LAB027 amplified the antitumor effect observed with oxaliplatin alone (−56% *versus* oxaliplatin-treated mice, $P<0.05$ at day 27).

***In vivo* effects of LAB027 on the toxicity of oxaliplatin and on the susceptibility of mice to bacterial**

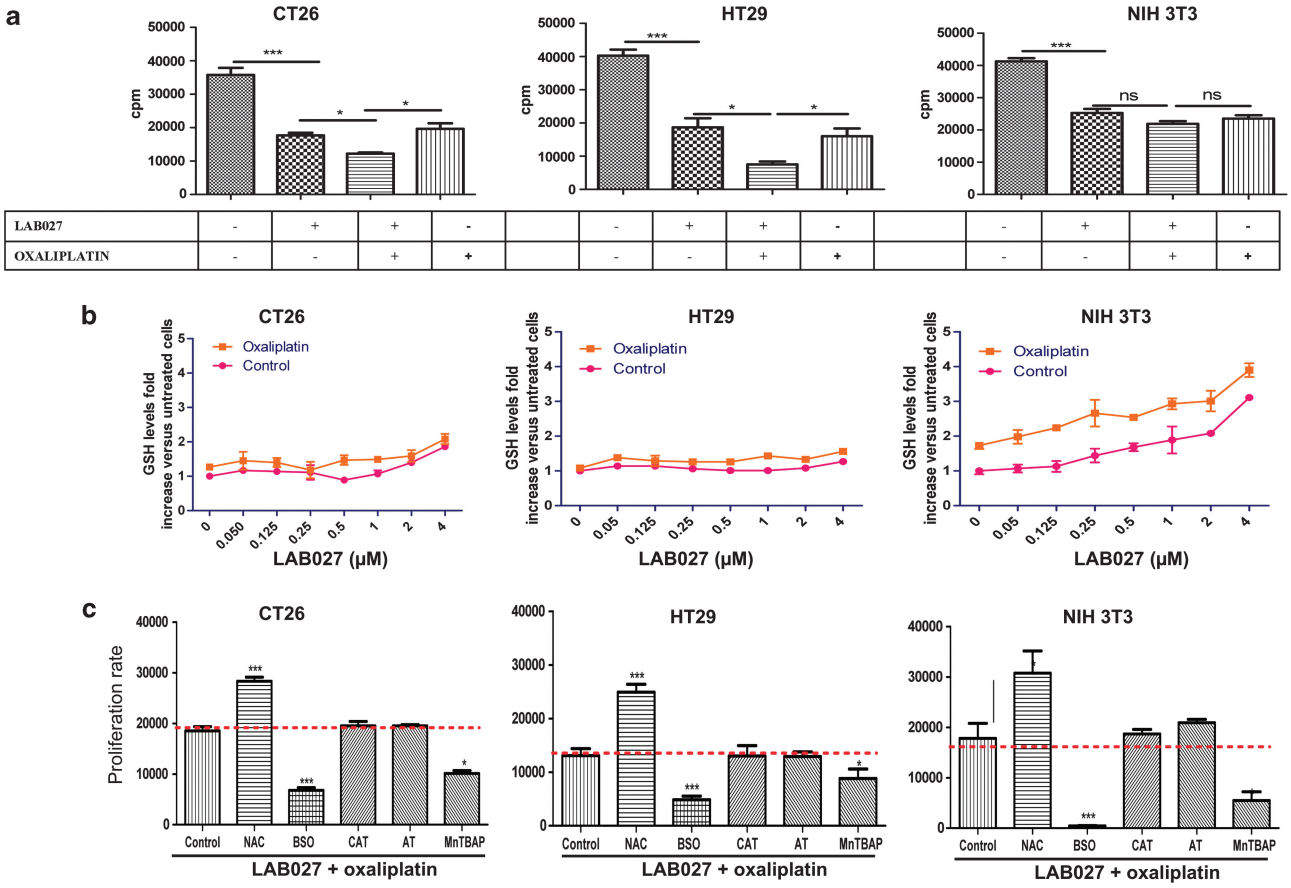

Figure 5 Proliferation (**a**) of CT26, HT29 and NIH3T3 cells treated with LAB027 alone or in association with oxaliplatin. Error bars represent S.E.M. LAB027 concentration was 1 μM for all the cells tested. Intracellular levels of reduced glutathione (**b**) in CT26 cells, HT29 cells and NIH3T3 cells treated with various concentrations of LAB027. Results are the mean ± S.E.M. of three experiments each performed in triplicate. Proliferation (**c**) of CT26, HT29 and NIH 3T3 cell lines following incubation with 1 μM LAB027 plus oxaliplatin alone, or associated with either 400 μM *N*-acetylcysteine, 400 μM DL-buthionine-[S,R]-sulfoximine (BSO), 200 μM 3-amino-1,2,4-triazole (AT), 50 units/ml catalase PEG (CAT) or with 100 μM MnTBAP. Oxaliplatin concentration was respectively 5, 0.5 and 5 μM for CT26, HT29 and NIH3T3 cells. Cellular proliferation was mesured by thymidine incorporation. Error bars represent S.E.M.

infection. We next investigated the effects of LAB027 on the toxicity of oxaliplatin in BALB/c mice. The toxicity on liver was evaluated by measuring serum concentrations of ALAT, LDH and alkaline phosphatases. Kidney function was assessed on serum BUN and creatinin (Supplementary Figure 4). None of these parameters were altered in the serum of mice treated with oxaliplatin or LAB027 alone, or in the serum of mice treated with both LAB027 and oxaliplatin. After 14 days the first injection of oxaliplatin, a significant decrease in the absolute numbers of peripheral leukocytes, neutrophils and platelets was observed *versus* control mice treated with PBS (Figure 6b). LAB027 alone had no hematological toxicity compared with untreated control mice. Furthermore, the administration of LAB027 in association with oxaliplatin significantly decreased the hematological toxicity of oxaliplatin. Indeed, the counts of peripheral leukocytes ($P=0.027$), neutrophils ($P=0.008$) and platelets ($P=0.035$) in the blood of mice treated with LAB027 and oxaliplatin were higher than in the blood of mice treated with oxaliplatin alone. Because bacterial infection is the main complication of neutropenia, the susceptibility of mice to intraperitoneal inoculation of *E. coli* was tested following the administration of oxaliplatin alone or in association with LAB027 (Figure 6c). In all, 40% of control mice treated with PBS survived 28 h after *E. coli* inoculation. However, no animal treated with oxaliplatin before *E. coli* inoculation, survived more than 22 h following the bacterial challenge. In contrast, 55% of mice treated with oxaliplatin and LAB027 survived 28 h following intraperitoneal inoculation of *E. coli* ($P=0.044$).

Discussion

This study provides pre-clinical evidence that the organotelluride catalyst LAB027, a prototypical member of family of the 'sensor/effector' multifunctional redox catalyst agents, is a new candidate molecule to treat colon cancer either alone or in combination with oxaliplatin.

Previous experiments have shown that 'sensor/effector' agents can act as cytotoxic molecules *in vitro*.[25] These agents are catalytic molecules that recognize a particular intracellular state of cells – such as an oxidative stress – and selectively kill the cells that are under this state. In our hands, tumor cells display an elevated basal level of ROS that is amplified by

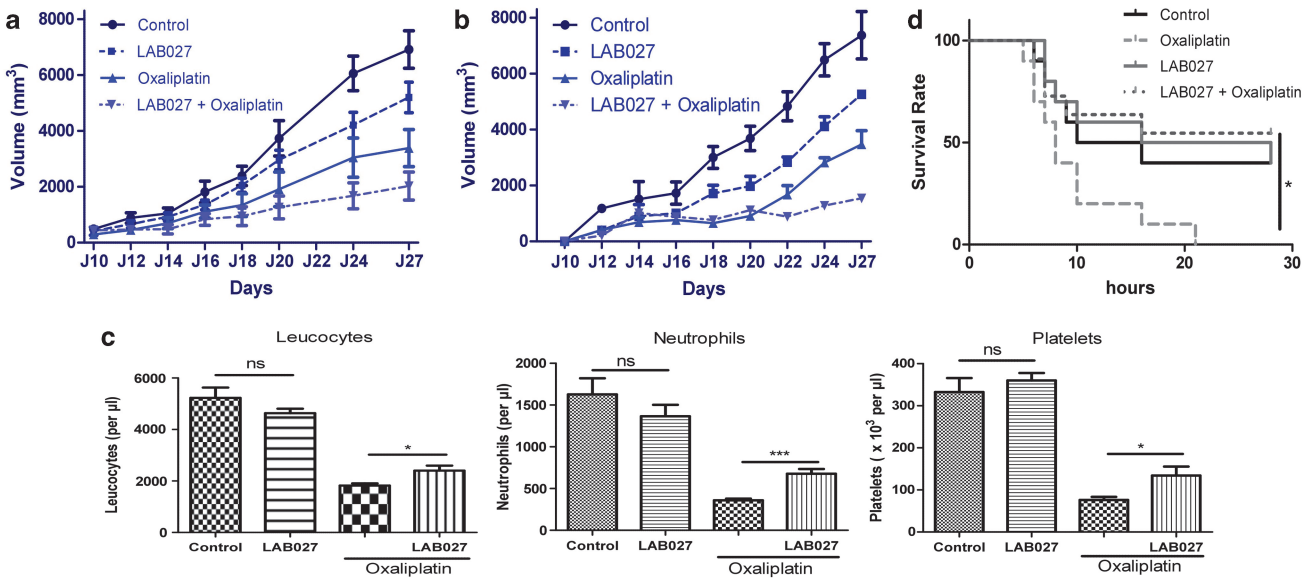

Figure 6 Tumor growth following implantation of 2×10^6 CT26 cells in BALB/c mice (**a**) or in SCID mice (**b**). Mice were treated as described in the 'Materials and Methods section' (seven mice/group). Biological toxicity (**c**): leukocytes, neutrophils and platelets count in the blood of mice on day 14, following two i.v. injections of oxaliplatin (10 mg/kg) on days 1 and 7 and two injections of LAB027 (10 mg/kg) on days 1 and 7. Survival rate of mice (**d**) following intraperitoneal injection of 10^7 *E. coli* in BALB/c mice. Mice were treated as described in the 'Material and Method section' (10 mice/group)

LAB027 to generate a lethal oxidative burst. The most likely explanation for this amplifying effect is an association of oxygen radical and H_2O_2 formation at the quinone and oxidation of cellular thiols catalyzed by tellurium in the presence of H_2O_2. Those chemical reactions are likely to increase the oxidative stress in tumor cells with a high initial level of H_2O_2, and ultimately push those cells over a critical 'life and death' (redox) threshold.[24] This also accounts for the differences of toxicity of the LAB027 compound in tumor and normal cells. Moreover in tumor cells, the levels of antioxidant enzyme activities are low and not modified by LAB027. In normal cells, the basal levels of antioxidant enzyme activities are higher and are still raised by LAB027, thus preventing cell death.[9] The differences between normal and tumor cells in terms of basal oxidative stress and antioxidant enzyme levels have already been used to selectively kill tumor cells *in vitro*. Thus, SOD mimics favor the dismutation of superoxide anions overproduced by tumor cells, and consecutively raise the production of H_2O_2 up to a cytotoxic level that is not reached in normal cells with low basal levels of H_2O_2.[9,16] The mechanism of action of LAB027 is different; it induces by itself an oxidative stress that is amplified by the pre-existing oxidative stress in tumor cells. H_2O_2 and not $O_2^{\bullet -}$ has a key role in the death induced by LAB027, as *N*-acetylcysteine but not the SOD mimic MnTBAP significantly decreases LAB027 toxicity. Incubation of LAB027 with the gamma-glutamylcysteine synthetase inhibitor BSO that depletes the cells in reduced glutathione significantly increases the cytotoxicity of LAB027 in all cell lines. By contrast, blocking catalase with amino-triazol or increasing its intracellular levels with PEG-catalase, has no effects on cell survival and proliferation whatever the cell type considered. These results indicate that H_2O_2-mediated LAB027 toxicity is controlled by the glutathione pathway rather than by the catalase pathway, as already observed with several chemotherapeutic drugs.

The role of ROS in tumor cell death induced by LAB027 is emphasized by the effects of the compound on the mitochondrial release of pro-apoptotic molecules. Members of the Bcl-2 family control the permeability of the mitochondrial outer membrane to various pro-apoptotic proteins.[26] In our hands, LAB027 exerts its powerful cytotoxic effect by inhibiting the expression of Bcl-2 and Bcl-xL, two antiapoptotic molecules, and increasing the expression of Bax and Bad, two pro-apoptotic molecules. This alteration in the mitochondrial membrane composition leads to the mitochondrial collapse, but is not followed by caspase-3 cleavage as usually observed during apoptosis.[26] Those results are in line with the ineffectiveness of caspase-3 inhibitors to abrogate LAB027-induced cell death and with the necrotic mode of death induced by LAB027 as demonstrated by YOPRO-1/PI staining of LAB027-treated cells. ROS have been reported to induce cell death by necrosis and/or apoptosis depending on the rate of ROS production, the duration of the oxidative burst and the cell type considered.[27] In our hands, LAB027 triggers a caspase-independent, ROS-mediated cell death by necrosis. LAB027 also induces an autophagic process as demonstrated by ATG-8 induction and cleavage, and by the phenomenon of vacuolization. Indeed, H_2O_2 can trigger the formation of autophagosomes through the oxidation of a critical cysteine residue on HsAtg4A. The resulting inactivation of HsAtg4A leads to the accumulation of Atg8-PE on the phagophore membrane and to the formation of autophagosomes.[28] However, it is not clear whether this mechanism is involved in cell death, or counteracts the toxic effects of LAB027 and favours cell survival by removal of harmful protein aggregates and damaged mitochondria, which are sources of altered proteins.[29]

The chemotherapeutic treatment of colon cancer usually requires the use of several drugs. Oxaliplatin is one of the most frequently used.[30,31] In our hands, the augmentation of

the antiproliferative effects of oxaliplatin on colon cancer cells when associated with LAB027, is linked to the increased intracellular concentration of H_2O_2. However, a similar increase in H_2O_2 concentration is observed in NIH3T3 fibroblasts treated by oxaliplatin and LAB027, and no antiproliferative effect is observed. This is explained by the increase in GSH levels that occurs in normal 3T3 fibroblasts but not in colon cancer cells. Because of its role in H_2O_2 detoxification, the glutathione pathway represents a major component of cellular defense against cytotoxic drugs as oxaliplatin These results are in agreement with the effect of LAB027 on glutathione reductase levels, an enzyme that restores the pool of reduced GSH and whose level is increased in normal but not in tumor cells. The role of glutathione reductase is also emphasized by the synergistic effect of the gamma-glutamylcysteine synthetase inhibitor BSO with LAB027 and oxaliplatin on tumor cells. The effect is still more dramatic on normal cells.

Thus, our data confirm that oxaliplatin exerts its anti-tumoral effects at least partly through the induction of an oxidative stress and emphasizes the role of reduced glutathione in the control of oxaliplatin cytotoxicity.[32] In tumor cells, high levels of reduced glutathione, the cofactor of glutathione peroxidase, have been associated with a multidrug resistance phenotype.[19] Compounds that target such protective mechanisms could enhance the activity of anticancer agents and reverse the multidrug resistance phenotype. For example, BSO, an inhibitor of glutathione synthesis, can increase the cytotoxicity of melphalan by preventing glutathione peroxidase activity and increasing H_2O_2 levels.[20] However, BSO depletes glutathione in both normal and cancer cells, which increases melphalan's hematological toxicity and prevents any enhancement of the therapeutic index of this anticancer agent.[33,34] Conversely, *N*-acetylcysteine protects normal cells from the cytotoxic effects of anticancer drugs by preventing the elevation of intracellular H_2O_2 through its reductive properties,[9] but abrogates the effectiveness of chemotherapeutic drugs. We have already observed that, as LAB027, mangafodipir prevents the hematological toxicity of oxaliplatin, but enhances its antitumoral activity against colon cancer both *in vitro* and *in vivo*.[16] The differential cytotoxic effects of mangafodipir on normal and cancer cells also result from differences in the redox status of those cells. Mangafodipir induces an overproduction of H_2O_2 through the dismutation of superoxide anions, but decreases the toxicity of H_2O_2 in normal cells through its glutathione reductase-like activity. Both mangafodipir and LAB027 increase the therapeutic index of oxaliplatin *in vitro* and *in vivo*, prevent hematologic toxicity and the death of animals injected with a lethal concentration of bacteria. Moreover, arsenic trioxide, one of the prototypical 'sensor/effector' chemotherapeutic agents, exerts its antitumoral activity through the induction of an oxidative burst without inducing leucopenia.[15]

Only a small number of studies have previously explored the antitumoral role of tellurium compounds. Only one tellurium-based compound, AS101, has been tested so far. AS101 (ammonium trichloro (dioxoethylene-O,O′) tellurate), a tellurium (IV) compound, is endowed with antitumor properties in several murine models.[35,36] Phase I clinical trials on patients with advanced cancer treated with AS101 have shown an increased production and secretion of a variety of cytokines, leading to a clear dominance of Th1 responses with a concurrent decrease in Th2 responses.[37] The predominance of Th1 responses is related to the antitumor activity of AS101. In addition, AS101, as a tellurium (IV) compound, can interact with thiols to form a Te-S bond. The ability of AS101 to interact with cysteine residue can alter protein functions,[38] increase intracellular ROS and favor the induction of apoptosis.[39] However, all the activities of AS101 are associated with little toxicity, and this drug is safe for clinical applications.[40]

The present study provides the first pre-clinical evidence that the organotelluride catalyst, LAB027 is a potential drug to treat colon cancer either alone or in combination with oxaliplatin through a mechanism that involves mainly necrosis. Tumor cell death is associated with the overproduction of intracellular ROS but with no elevation of reduced glutathione levels as observed in normal cells. This difference may explain the limited kidney, liver and hematological toxicity of this compound *in vivo*. Finally, this report shows for the first time that 'sensor/effector' pro-oxidative agents could represent effective and safe options to treat patients with colon cancer.

Materials and Methods

Animals. BALB/c and BALB/c SCID female mice between 6 and 8 weeks of age were used in all experiments (Harlan, Gannat, France). All mice were housed in autoclaved cages with sterile food and water. Animals received humane care in compliance with institutional guidelines.

LAB027 synthesis. The synthesis of LAB027 is described in detail in Supplementary files (Supplementary data and Supplementary Figure 1).

Chemicals, cell lines and culture. All chemicals were from Sigma (Saint Quentin Fallavier, France) except for oxaliplatin (Eloxatine, Sanofi-Pharma, Paris, France). CT26 (mouse colon carcinoma), HT29 (human colon carcinoma), NIH 3T3 (mouse fibroblast) and W138 (human lung fibroblast) were obtained from American Type Culture Collection (Manassas, VA, USA). All cell lines were cultured in DMEM/glutamax-I supplemented with 10% heat-inactivated FCS and antibiotics (Life Technologies, Cergy Pontoise, France). All cell lines were routinely tested for Mycoplasma infection.

Cellular production of $O_2^{\bullet -}$ and H_2O_2. Cells (2×10^4 cells/well) were seeded in 96-well plates (Costar, Corning, Inc., Corning, NY) and incubated for 48 h in culture medium alone or added with various concentrations of LAB027 alone or in combination with oxaliplatin. Levels of intracellular superoxide anion $O_2^{\bullet -}$ and H_2O_2 were assessed spectrofluorometrically (Packard Bioscience, Boston, MA, USA) by oxidation of dihydroethidium (DHE) (Molecular Probes, Leiden, The Netherlands) and of 2′,7′-dichlorodihydrofluorescein diacetate (H_2DCFDA) (Molecular Probes), respectively, as previously described.[16] The levels of $O_2^{\bullet -}$ or H_2O_2 were calculated in each sample as follows: ROS rate (arbitrary units/min/10^6 cells) = (fluorescence intensity (arbitrary units) at T60 minutes − fluorescence intensity (arbitrary units) at T0)/60 min/number of viable cells as measured by the crystal violet assay.

Determination of enzymatic activities. The SOD activity in tumor or normal cells was evaluated by the method of Beauchamp and Fridovich[30] and expressed as units/10^6 cells. The catalase activity in tumor or normal cells was determined according to Aebi[41] and expressed as units/10^6 cells. The glutathione reductase assay was performed by the method of Carlberg and Mannervik[42] and expressed as nmol/min/10^6 cells. Levels of extracellular GSH were measured by the method of Baker *et al*.[43] and expressed as nmol/10^6 cells.

***In vitro* cell proliferation and viability assays.** CT26, HT29, NIH 3T3 or W138 cells (2×10^4 cells/well) were seeded into 96-well plates and incubated for

48 h in complete DMEM medium with varying amounts of LAB027 alone or with oxaliplatin. Cell proliferation was determined by pulsing the cells with [^{3}H] thymidine (1 μCi/well) during the last 16 h of culture. Cell viability was evaluated by the crystal violet assay.[16] Results are expressed as percentages of viable cells compared with untreated cells (that have 100% viability).

Levels of intracellular and extracellular reduced glutathione. The levels of intracellular glutathione were assessed spectrofluorometrically by monochlorobimane staining.[44] Briefly, tumor cells (2×10^4/well) or normal NIH3T3 (2×10^4/well) were seeded in 96-well plates and incubated for 48 h in complete medium with LAB027 alone or in combination with oxaliplatin at concentrations described in figure legends. Cells were washed once with PBS and then incubated with 50 μM monochlorobimane in PBS. The fluorescence intensity was measured after 15 min at 37°C. Excitation and emission wavelengths were 380 and 485 nm, respectively. The intracellular glutathione level was expressed as arbitrary units of fluorescence intensity/number of adherent cells as measured by the crystal violet assay. Extracellular reduced glutathione was assayed in culture supernatants using the method of Baker *et al.*[43]

Immunoblotting of cell lysates. HT29 cells were treated or not with 1, 2 or 4 μM LAB027 for 24 h then lysed in ice-cold RIPA.[9] Protein (50 μg) extracts were analyzed by immunoblotting after 10–15% SDS-PAGE using of rabbit polyclonal anti-mouse pro- and active caspase-3 (1 : 1500, Abcam 47131, Paris, France), rabbit polyclonal anti-mouse caspase-8, mouse polyclonal anti-mouse Bcl-2, Bcl-xL and Bax primary antibodies (1 : 200, Santa Cruz Biotechnology, Inc., Santa Cruz, CA, USA), Bad primary antibody (1 : 100, Santa Cruz Biotechnology), ATG-8 primary antibody (1 : 500, Sigma-Aldrich, Saint-Quentin Fallavier, France) and mouse monoclonal anti-β-actin (1 : 50 000, Sigma). After washing, membranes were incubated with a 1 : 1000 goat anti-rabbit or goat anti-mouse secondary antibody (Sigma-Aldrich). The membranes were developed in Super Signal West Pico Chemiluminescent Substrate (Pierce, CO, USA). Images of blots were obtained using Fujifilm LAS3000 digital imager analyzed with Fujifilm Multi-Gauge Imaging software (Fujifilm, Tokyo, Japan).

Modulation of the catalase and glutathione reductase pathways. HT29, CT26, NIH 3T3 or W138 cells (2×10^4 cells/well) were pre-incubated for 2 h with either 400 μmol/l *N*-acetyl cysteine (NAC), or with 50 units/ml PEG-catalase, or with 200 μmol/l aminotriazol (ATZ, a catalase inhibitor) or with 400 μmol/l *L*-buthionine-SR-sulfoximine (BSO, a gamma-glutamylcysteine synthetase inhibitor). Those concentrations were chosen because they significantly modulated either reduced glutathione concentration (BSO, NAC) or catalase activity (PEG-catalase, ATZ) (not shown). The cells were then incubated with 1 μM LAB027 alone or in combination with oxaliplatin for 48 h. Cell proliferation was assayed by pulsing the cells with [^{3}H] thymidine (1 μCi/well) during the last 16 h of culture.

Study of caspase inhibition. HT29 cells (2×10^4 cells/well) were pre-incubated for 2 h with either 40 μM caspase-3-specific inhibitor Ac-DEVD-FMK or with 40 μM caspase-8 inhibitor Z-IETD-FMK, or with the broad-spectrum 40 μM caspase inhibitor Z-VAD-FMK. The cells were then incubated with LAB027 for 48 h. Cell viability was evaluated by the crystal violet assay. Results are expressed as percentages of viable cells compared with untreated cells (100% viability).

Fluorescence-activated cell sorting analysis of cell death. Apoptosis and necrosis were analyzed by the fluorescence-activated cell sorting (FACS) Canto II flow cytometer (Becton Dickinson, Franklin Lakes, NJ, USA), using the Membrane Permeability/Dead Cell Apoptosis Kit with YO-PRO-1 and Propidium iodide (PI) for Flow Cytometry (Invitrogen, Cergy Pontoise, France) under the manufacturer's recommendations. Briefly, 5×10^5 HT29 cells were incubated with 4 μM LAB027 for a period of time indicated in the legends of figures. After the incubation period, cells were collected and stained for 30 min on ice with 1.5 μM PI and 0.1 μM YO-PRO-1. Cells were washed two times and analyzed by flow cytometry.

Acridine orange staining for autophagy detection. Acridine orange (Sigma) staining was performed according to Kanzawa *et al.*[45] Briefly, HT29 cells were treated or not for 24 h with 4 μM LAB027. After the incubation period, cells were washed twice with phosphate-buffered saline and stained with 1 μM acridine orange for 15 min at 37°C. Cells were washed and analyzed by fluorescence microscopy using 490-nm band-pass blue excitation filters and a 515-nm long-pass barrier filter.

***In vivo* antitumor activity of LAB027.** CT26 (2×10^6) cells were injected subcutaneously into the back of BALB/c or BALB/c SCID mice. When the tumors reached a mean size of 200–500 mm^3, mice were randomized (day 10) in each experimental and control groups depending on tumor size, in order to start the treatment with a similar mean size in each group. One group of seven mice was treated by intraperitoneal oxaliplatin (10 mg/kg/week) starting on day 10. One group of seven mice was treated by intravenous LAB027 (10 mg/kg/week) starting on day 10. One group of seven mice was treated with intravenous LAB027 (10 mg/kg/week) and intraperitoneal oxaliplatin (10 mg/kg/week) starting on day 10. One control group of seven mice was injected with PBS. Tumor size was measured with a calliper rule every 2 days. Tumor volume was calculated as follows: TV (mm^3) = (L $\times$ W^2)/2, where L is the longest and W the shortest radius of the tumor in millimeters. Results were expressed as means of tumor volumes ± S.E.M. ($n = 7$ in each group).

***In vivo* analysis of blood, liver and kidney toxicity.** Mice were injected with PBS alone or intraperitoneal, oxaliplatin alone, or intravenous LAB027 alone or intraperitoneal oxaliplatin in association with intravenous LAB027 at days 0 and 7. Five mice were treated in each group. After 14 days of the first injection, mice were killed by cervical dislocation. Blood samples were then collected from each mouse. Leukocytes, neutrophils and platelets were enumerated using a Malassez cell after hypotonic red blood cell lysis. Liver enzymes ALAT, LDH, alkaline phosphatases, BUN and creatinine were assayed using a multiparametric analyzer (Hitachi 747, Roche Diagnostics, Meylan, France).

Susceptibility of mice to bacterial infection. BALB/c female mice were injected with vehicle alone (PBS), or intraperitoneal oxaliplatin alone, or intravenous LAB027 alone or intraperitoneal oxaliplatin and intravenous LAB027 days 0 and seven. Five mice were treated in each group. After 14 days of the first injection, mice were injected i.p with a lethal dose of 10^7 *E. coli* on day 9. The survival rate of mice was evaluated during 24 h following *E. coli* injection. A total of 10 mice were treated in each group in two independent experiments.

Statistical analysis. The statistical significance of differences between experimental treated groups and untreated controls was analyzed by Student's *t*-test for comparison of means. A level of $P < 0.05$ was accepted as significant. $^*P < 0.05$; $^{***}P < 0.01$ *versus* controls.

Conflict of Interest

The authors declare no conflict of interest.

Acknowledgements. This research has been funded by a grant from the European Community's Seventh Framework Program (FP7/2007-2013) under grant agreement no (215009). The authors thank Ms Agnes Colle for editing the manuscript and Ms Marie Mianowski for reviewing the manuscript.

1. Halliwell B, Gutteridge JM. *Free Radicals in Biology and Medicine.* Oxford University Press: UK, 2007.
2. Benhar M, Engelberg D, Levitzki A. ROS, stress-activated kinases and stress signaling in cancer. *EMBO Rep* 2002; **3**: 420–425.
3. Burdon RH. Superoxide and hydrogen peroxide in relation to mammalian cell proliferation. *Free Radic Biol Med* 1995; **18**: 775–794.
4. Murrell GA, Francis MJ, Bromley L. Modulation of fibroblast proliferation by oxygen free radicals. *Biochem J* 1990; **265**: 659–665.
5. Bae YS, Kang SW, Seo MS, Baines IC, Tekle E, Chock PB *et al.* Epidermal growth factor (EGF)-induced generation of hydrogen peroxide. Role in EGF receptor-mediated tyrosine phosphorylation. *J Biol Chem* 1997; **272**: 217–221.
6. Sundaresan M, Yu ZX, Ferrans VJ, Irani K, Finkel T. Requirement for generation of H2O2 for platelet-derived growth factor signal transduction. *Science (New York, NY)* 1995; **270**: 296–299.
7. Jackson AL, Loeb LA. The contribution of endogenous sources of DNA damage to the multiple mutations in cancer. *Mutat Res* 2001; **477**: 7–21.
8. Gupta A, Rosenberger SF, Bowden GT. Increased ROS levels contribute to elevated transcription factor and MAP kinase activities in malignantly progressed mouse keratinocyte cell lines. *Carcinogenesis* 1999; **20**: 2063–2073.

9. Laurent A, Nicco C, Chereau C, Goulvestre C, Alexandre J, Alves A *et al.* Controlling tumor growth by modulating endogenous production of reactive oxygen species. *Cancer Res* 2005; **65**: 948–956.
10. Mates JM, Segura JA, Alonso FJ, Marquez J. Intracellular redox status and oxidative stress: implications for cell proliferation, apoptosis, and carcinogenesis. *Arch Toxicol* 2008; **82**: 273–299.
11. Oberley TD, Oberley LW. Antioxidant enzyme levels in cancer. *Histol Histopathol* 1997; **12**: 525–535.
12. Benhar M, Dalyot I, Engelberg D, Levitzki A. Enhanced ROS production in oncogenically transformed cells potentiates c-Jun N-terminal kinase and p38 mitogenactivated protein kinase activation and sensitization to genotoxic stress. *Mol Cell Biol* 2001; **21**: 6913–6926.
13. Jabs T. Reactive oxygen intermediates as mediators of programmed cell death in plants and animals. *Biochem Pharmacol* 1999; **57**: 231–245.
14. Hwang PM, Bunz F, Yu J, Rago C, Chan TA, Murphy MP *et al.* Ferredoxin reductase affects p53-dependent, 5-fluorouracil-induced apoptosis in colorectal cancer cells. *Nat Med* 2001; **7**: 1111–1117.
15. Jing Y, Dai J, Chalmers-Redman RM, Tatton WG, Waxman S. Arsenic trioxide selectively induces acute promyelocytic leukemia cell apoptosis via a hydrogen peroxide-dependent pathway. *Blood* 1999; **94**: 2102–2111.
16. Alexandre J, Nicco C, Chereau C, Laurent A, Weill B, Goldwasser F *et al.* Improvement of the therapeutic index of anticancer drugs by the superoxide dismutase mimic mangafodipir. *J Natl Cancer Inst* 2006; **98**: 236–244.
17. Hussain SP, Amstad P, He P, Robles A, Lupold S, Kaneko I *et al.* p53-induced up-regulation of MnSOD and GPx but not catalase increases oxidative stress and apoptosis. *Cancer Res* 2004; **64**: 2350–2356.
18. Trachootham D, Alexandre J, Huang P. Targeting cancer cells by ROS-mediated mechanisms: a radical therapeutic approach? *Nat Rev* 2009; **8**: 579–591.
19. Hamaguchi K, Godwin AK, Yakushiji M, O'Dwyer PJ, Ozols RF, Hamilton TC. Cross-resistance to diverse drugs is associated with primary cisplatin resistance in ovarian cancer cell lines. *Cancer Res* 1993; **53**: 5225–5232.
20. Skapek SX, Colvin OM, Griffith OW, Elion GB, Bigner DD, Friedman HS. Enhanced melphalan cytotoxicity following buthionine sulfoximine-mediated glutathione depletion in a human medulloblastoma xenograft in athymic mice. *Cancer Res* 1988; **48**: 2764–2767.
21. Cullen JJ, Weydert C, Hinkhouse MM, Ritchie J, Domann FE, Spitz D *et al.* The role of manganese superoxide dismutase in the growth of pancreatic adenocarcinoma. *Cancer Res* 2003; **63**: 1297–1303.
22. Zhang Y, Zhao W, Zhang HJ, Domann FE, Oberley LW. Overexpression of copper zinc superoxide dismutase suppresses human glioma cell growth. *Cancer Res* 2002; **62**: 1205–1212.
23. Hileman EO, Liu J, Albitar M, Keating MJ, Huang P. Intrinsic oxidative stress in cancer cells: a biochemical basis for therapeutic selectivity. *Cancer Chemother Pharmacol* 2004; **53**: 209–219.
24. Mecklenburg S, Shaaban S, Ba LA, Burkholz T, Schneider T, Diesel B *et al.* Exploring synthetic avenues for the effective synthesis of selenium- and tellurium-containing multifunctional redox agents. *Org Biomol Chem* 2009; **7**: 4753–4762.
25. Shabaan S, Ba LA, Abbas M, Burkholz T, Denkert A, Gohr A *et al.* Multicomponent reactions for the synthesis of multifunctional agents with activity against cancer cells. *Chem Commun (Camb, England)* 2009; **40**: 4702–4704.
26. Joza N, Kroemer G, Penninger JM. Genetic analysis of the mammalian cell death machinery. *Trends Genet* 2002; **18**: 142–149.
27. Orrenius S, Gogvadze V, Zhivotovsky B. Mitochondrial oxidative stress: implications for cell death. *Annu Rev Pharmacol Toxicol* 2007; **47**: 143–183.
28. Scherz-Shouval R, Shvets E, Fass E, Shorer H, Gil L, Elazar Z. Reactive oxygen species are essential for autophagy and specifically regulate the activity of Atg4. *EMBO J* 2007; **26**: 1749–1760.
29. Azad MB, Chen Y, Gibson SB. Regulation of autophagy by reactive oxygen species (ROS): implications for cancer progression and treatment. *Antioxid Redox Signal* 2009; **11**: 777–790.
30. Beauchamp C, Fridovich I. Superoxide dismutase: improved assays and an assay applicable to acrylamide gels. *Anal Biochem* 1971; **44**: 276–287.
31. Diaz-Rubio E, Sastre J, Zaniboni A, Labianca R, Cortes-Funes H, de Braud F *et al.* Oxaliplatin as single agent in previously untreated colorectal carcinoma patients: a phase II multicentric study. *Ann Oncol* 1998; **9**: 105–108.
32. Godwin AK, Meister A, O'Dwyer PJ, Huang CS, Hamilton TC, Anderson ME. High resistance to cisplatin in human ovarian cancer cell lines is associated with marked increase of glutathione synthesis. *Proc Natl Acad Sci U S A* 1992; **89**: 3070–3074.
33. Bailey HH, Mulcahy RT, Tutsch KD, Arzoomanian RZ, Alberti D, Tombes MB *et al.* Phase I clinical trial of intravenous L-buthionine sulfoximine and melphalan: an attempt at modulation of glutathione. *J Clin Oncol* 1994; **12**: 194–205.
34. Bailey HH, Ripple G, Tutsch KD, Arzoomanian RZ, Alberti D, Feierabend C *et al.* Phase I study of continuous-infusion L-SR-buthionine sulfoximine with intravenous melphalan. *J Natl Cancer Inst* 1997; **89**: 1789–1796.
35. Hayun M, Naor Y, Weil M, Albeck M, Peled A, Don J *et al.* The immunomodulator AS101 induces growth arrest and apoptosis in multiple myeloma: association with the Akt/survivin pathway. *Biochem Pharmacol* 2006; **72**: 1423–1431.
36. Sredni B, Caspi RR, Klein A, Kalechman Y, Danziger Y, Ben Ya'akov M *et al.* A new immunomodulating compound (AS-101) with potential therapeutic application. *Nature* 1987; **330**: 173–176.
37. Sredni B, Tichler T, Shani A, Catane R, Kaufman B, Strassmann G *et al.* Predominance of TH1 response in tumor-bearing mice and cancer patients treated with AS101. *J Natl Cancer Inst* 1996; **88**: 1276–1284.
38. Okun E, Dikshtein Y, Carmely A, Saida H, Frei G, Sela BA *et al.* The organotellurium compound ammonium trichloro(dioxoethylene-o,o′)tellurate reacts with homocysteine to form homocystine and decreases homocysteine levels in hyperhomocysteinemic mice. *FEBS J* 2007; **274**: 3159–3170.
39. Frei GM, Kremer M, Hanschmann KM, Krause S, Albeck M, Sredni B *et al.* Antitumour effects in mycosis fungoides of the immunomodulatory, tellurium-based compound AS101. *Br J Dermatol* 2008; **158**: 578–586.
40. Sredni B, Xu RH, Albeck M, Gafter U, Gal R, Shani A *et al.* The protective role of the immunomodulator AS101 against chemotherapy-induced alopecia studies on human and animal models. *Int J Cancer* 1996; **65**: 97–103.
41. Aebi H. Catalase *in vitro*. *Methods Enzymol* 1984; **105**: 121–126.
42. Carlberg I, Mannervik B. Glutathione reductase. *Methods Enzymol* 1985; **113**: 484–490.
43. Baker MA, Cerniglia GJ, Zaman A. Microtiter plate assay for the measurement of glutathione and glutathione disulfide in large numbers of biological samples. *Anal Biochem* 1990; **190**: 360–365.
44. Rice GC, Bump EA, Shrieve DC, Lee W, Kovacs M. Quantitative analysis of cellular glutathione by flow cytometry utilizing monochlorobimane: some applications to radiation and drug resistance *in vitro* and *in vivo*. *Cancer Res* 1986; **46**: 6105–6110.
45. Kanzawa T, Kondo Y, Ito H, Kondo S, Germano I. Induction of autophagic cell death in malignant glioma cells by arsenic trioxide. *Cancer Res* 2003; **63**: 2103–2108.

Supplementary Information accompanies the paper on Cell Death and Disease website (http://www.nature.com/cddis)